

A formulation for reliable estimation of active crustal deformation and its application to central Greece

Constantinos B. Papazachos and Anastasia A. Kiratzi

Geophysical Laboratory, University of Thessaloniki, Mail Box 352-1, GR-540 06 Thessaloniki, Greece

Accepted 1992 May 13. Received 1992 March 23; in original form 1991 December 30

SUMMARY

A procedure for the analysis of data, concerning seismic moment release and fault-plane solutions, for the estimation of active crustal deformation is proposed. The formulation takes advantage of all the available historical and instrumental data for the calculation of the 'size' of the deformation in a seismic zone and of all the reliable fault-plane solutions which are available for a broader seismic belt for the determination of the 'shape' of the deformation. A detailed analysis of the errors involved in each parameter, based on a Monte Carlo numerical method, is suggested. The proposed procedure is applied to a region of extensional tectonics in central Greece. The resulting seismic strain rates show that the dominant mode of deformation in the area is extension at a rate of the order of 6 mm yr^{-1} and a mean azimuth of N25°W. A vertical contraction rate of about 1 mm yr^{-1} has also been calculated. The results from geodetic measurements performed by Billiris *et al.* (1991) declare that the calculated seismic deformation represents about 60 per cent of the total strain of this area.

Key words: crustal deformation, fault-plane solution, Greece, seismic moment, strain.

1 INTRODUCTION

The method of analysis that is usually applied for the estimation of active crustal deformation requires the knowledge of both the fault-plane solution (strike, dip, rake) and the seismic moment for each earthquake of a data sample complete over a certain magnitude threshold (Tselentis & Makropoulos 1986; Jackson & McKenzie 1988a,b; Ekstrom & England 1989). Bearing in mind that reliable fault-plane solutions exist only for recent large earthquakes, this method of analysis is applicable to an observational period of 30 yr. It is possible to extend this period back in time, by assuming the fault parameters of the past events, and this has been done by some researchers (Jackson & McKenzie 1988a,b; Ambraseys & Jackson 1990; Papazachos *et al.* 1990; Kiratzi 1991; Taymaz, Jackson & McKenzie 1991). Anyhow, no matter how well justified these assumptions are, it is very likely that they introduce considerable error and bias. The fact that the known past earthquakes usually have a large magnitude makes the situation more difficult and leads to controversial results. One such example is the application of this method to the Aegean Sea and the surrounding area where values from a few millimetres to some centimetres per year have been

determined for the maximum velocity rate by different researchers.

To overcome the previously mentioned drawbacks, a method of analysis is suggested which permits:

(a) the use of all available complete data, which include information on smaller recent shocks and on strong instrumental and historical earthquakes of a much longer period, for the seismic moment rate calculation in a seismic zone; and

(b) the use of fault parameters deduced from reliable fault-plane solutions of recent strong earthquakes and from reliable field observations of past strong earthquakes which occurred in a broader seismic belt.

The errors involved in the determination of active crustal deformation is also an important problem (Jackson & McKenzie 1988a,b; Ekstrom & England 1989). For this reason, a detailed analysis of these errors is also performed in the present study.

This procedure of data analysis for the estimation of parameters related to active crustal deformation (strain rates, velocities, etc) and the corresponding procedure of

error estimation is applied to three seismic zones of central Greece.

2 THE METHOD FOR ANALYSIS OF DATA

Let us assume that we have a seismic zone with known dimensions (length l_1 , width l_2 and depth extend l_3). If all deformation that occurs in the volume V of the zone is seismic then Kostrov (1974) showed that the strain rate tensor $\dot{\epsilon}_{ij}$ can be calculated using the following relationship:

$$\dot{\epsilon}_{ij} = \frac{1}{2\mu V \tau} \sum_{n=1}^N M_{ij}^n \quad (1)$$

where μ is the shear modulus and M_{ij}^n are the elements of the moment tensor of the n th earthquake out of N earthquakes which occurred over a τ time interval.

We now choose a coordinate system with the horizontal axes, x_1 and x_2 , parallel and normal to the trend of the zone, respectively, and the vertical axis, x_3 , going downwards. Following the formulation developed in Jackson & McKenzie (1988a) we can now calculate the elements of the velocity tensor, U_{ij} , as follows:

$$\begin{aligned} U_{ii} &= \frac{1}{2\mu \tau l_k l_j} \sum_{n=1}^N M_{ii}^n \quad i = 1, 2, 3 \quad k \neq j, i \neq k, j \neq i \\ U_{12} &= \frac{1}{\mu \tau l_1 l_3} \sum_{n=1}^N M_{12}^n \\ U_{i3} &= \frac{1}{\mu \tau l_1 l_2} \sum_{n=1}^N M_{i3}^n \quad i = 1, 2. \end{aligned} \quad (2)$$

Jackson & McKenzie (1988a) quote some restrictions to the validity of equations (2). They discuss that these formulae hold for U_{13} and U_{23} if the zone's vertical dimension, l_3 , is much smaller than the horizontal ones l_1 and l_2 (which is usually the case) and for U_{12} only if the zone's length, l_1 , is much greater than its width, l_2 . In practice, though, the fulfilment of these restrictive theoretical demands is much less important than the fact that for short time periods the internal deformation does not result from forces applied at the boundaries of the zone. The use of data of a long time period is required so that any deformation in the zone might be reflected in the seismicity.

The elements of M^n are calculated using the relation:

$$M^n = M_0^n (\bar{\mathbf{u}} \cdot \bar{\mathbf{n}} + \bar{\mathbf{n}} \cdot \bar{\mathbf{u}}) = M_0^n F^n, \quad (3)$$

where M_0 is the scalar seismic moment and $\bar{\mathbf{u}}$ and $\bar{\mathbf{n}}$ are unit vectors parallel to the slip vector and normal to the fault plane, respectively. It can be proved that:

$$F^n = \bar{\mathbf{u}} \cdot \bar{\mathbf{n}} + \bar{\mathbf{n}} \cdot \bar{\mathbf{u}}$$

is a function of the strike, ϕ , of the dip, δ , and of the rake, λ , of the earthquake (Aki & Richards 1980). M_0 is computed either directly from the seismograms or using an empirical moment—magnitude relation of the form:

$$\log M_0 = cM_s + d, \quad (4)$$

where M_s is the surface wave magnitude and c and d are constants.

Using equations (1)–(4) we can calculate the velocity tensor if we know the magnitudes and the fault-plane solutions of N earthquakes which occurred over a period of τ years. The main weakness of this procedure lies in the calculation of M^n using equation (3). As can be easily seen, equation (3) consists of two parts: M_0^n which represents the 'size' of the earthquake and F^n which is a 'shape' tensor representing the 'geometrical' features of the earthquake.

We want to rewrite equation (3) for the annual rates of the whole zone. This means that if we have the annual moment rate tensor, \dot{M} , and the scalar annual moment rate, \dot{M}_0 , we want to find, \bar{F} , an average 'shape' tensor of the zone, i.e. a *representative focal mechanism tensor* which is supposed to be constant over time. Then, the following relation holds:

$$\dot{M} = (\dot{M}_0 \cdot \bar{F}) = \dot{M}_0 \cdot \bar{F}, \quad (5)$$

where

$$\bar{F} = \frac{\dot{M}}{\dot{M}_0} = \frac{\sum_{n=1}^N M^n / \tau}{\sum_{n=1}^N M_0^n / \tau} = \frac{\sum_{n=1}^N M^n}{\sum_{n=1}^N M_0^n} = \frac{\sum_{n=1}^N M_0^n F^n}{\sum_{n=1}^N M_0^n}. \quad (6)$$

The problem that we mentioned before lies in the fact that we usually have only a few earthquakes with known fault-plane solutions for each zone, which have occurred over a short period of time. Hence, the determination of \dot{M}_0 and \bar{F} from this data is poor. We attempt to overcome this problem in two steps.

(a) We group the zones with similar tectonic features (e.g. fault plane solutions) in big *belts* and calculate \bar{F} for each belt by relation (6). In this case, N is the number of earthquakes of each belt for which reliable solutions are available, regardless of the time in which they occurred or the completeness of the data. Thus, we increase the number of fault-plane solutions used for the estimation of \bar{F} for each zone.

(b) \dot{M}_0 in equation (5) is not calculated by the few earthquakes with known focal mechanisms of each zone which occurred (and have to be complete) in a short time period. Rather, we take advantage of the whole data set of earthquakes (instrumental and historical) that occurred in the zone over a much longer period of time. We use this data set to calculate the parameters a and b of the Gutenberg–Richter relation and then determine \dot{M}_0 using the formulation of Molnar (1979) as will be described later.

Equations (1) and (2) are now equivalent to:

$$\dot{\epsilon}_{ij} = \frac{1}{2\mu V} \dot{M}_{ij}, \quad (7)$$

$$U_{ii} = \frac{1}{2\mu l_k l_j} \dot{M}_{ii} \quad i = 1, 2, 3 \quad k \neq i, i \neq j, j \neq k, \quad (8)$$

$$U_{12} = \frac{1}{\mu l_1 l_3} \dot{M}_{12}, \quad (9)$$

$$U_{i3} = \frac{1}{\mu l_1 l_2} \dot{M}_{i3} \quad i = 1, 2. \quad (10)$$

Thus, in order to determine the deformation rates within a seismic zone, the following procedure is applied.

At first, we determine \bar{F} for each belt (equations 4 and 6) and \dot{M}_0 (equation 14) in order to calculate \dot{M} (equation 5) in the North–East–Down coordinate system. We perform a tensor rotation into the zone system $Ox_1x_2x_3$. Using (7)–(10) we calculate the strain rate tensor, $\dot{\epsilon}$, and the velocity tensor, U . Since we prefer the eigensystem configuration of U , we calculate its eigenvalues and the direction angles of its eigenvectors.

In order to calculate the rate of the seismic moment release in a seismic zone, the methodology proposed by Molnar (1979) was applied. Starting from the Gutenberg–Richter empirical expression, which relates the recurrence of events with different magnitudes, and using another empirical relation between magnitude and seismic moment, the relative number of events with seismic moment greater or equal to M_0 is given by the relation:

$$N(M_0) = A \cdot M_0^{-B}, \quad (11)$$

where

$$A = 10^{[a+(bd/c)]} \quad \text{and} \quad B = \frac{b}{c}, \quad (12)$$

where a , b are the constants of the Gutenberg–Richter relation

$$\log N = a - bM, \quad (13)$$

and c , d the constants of the empirical moment–magnitude relation (equation 4). The rate of occurrence of seismic moment, \dot{M}_0 , is then given by the relation:

$$\dot{M}_0 = \frac{A}{1-B} \cdot M_{0,\max}^{(1-B)}, \quad (14)$$

where $M_{0,\max}$ is the seismic moment released by the maximum earthquake in the zone.

The calculation of the constants a and b (equation 3) is performed by a method which some seismologists call the ‘mean value method’ (Milne & Davenport 1969). This method is described in detail in Papazachos (1990). By this method we can use several sets of complete data for each zone and calculate the annual frequencies of earthquakes for a large range of magnitudes. In this way, we make full use of the information concerning present century and historical strong earthquakes and instrumental information of small recent earthquakes.

It has been observed by various researchers (i.e. Scholz 1968) that large events do not fall on the b -curve, but occur more frequently. In this case the use of equation (14) might lead to biased estimations of the moment rate. For this reason we checked the residuals of the large earthquakes from the b -curves for the whole Aegean area, as this was separated by Papazachos (1990). We did not observe any tendency for systematic deviation for these events from the b -curves but the residuals follow a normal distribution with a zero mean. Hence, the application of equation (14), at least for the Aegean area, is expected to give reliable estimation for the moment rate.

3 ERROR ANALYSIS

A detailed error analysis has to take into account all possible random errors of the parameters used in the

calculations. Usually these errors are considered to have a Gaussian probability density, and error analysis is based on the transmission of small fluctuations of the input parameters through the model to the output results. Usually, only first-order error terms are used in the analysis. The problem of this procedure is that for non-linear models the errors in the output parameters are not Gaussian, i.e. in models with a high degree of non-linearity, high-order error terms cannot be neglected. One way to overcome this problem is to directly simulate the problem using a Monte Carlo technique.

In the present study errors are introduced to our final results in equations (7)–(10), mainly through \dot{M} . From equation (5) we can see that errors in \dot{M} are caused by errors in M_0 and \bar{F} . We will examine these errors separately.

3.1 Errors in \dot{M}_0

From equation (14) it is obvious that errors in \dot{M}_0 are due to errors in A , B and $M_{0,\max}$ and finally through equations (4) and (12) to errors in a , b , c , d and $M_{s,\max}$. If we assume that we have random errors in these parameters with known medians and standard deviations we can introduce Gaussian deviation in them and, through equations (4), (12) and (14), estimate a new value for \dot{M}_0 . Unfortunately our input parameters are correlated, i.e. the covariance matrix, \mathbf{V} , of the parameter vector $\mathbf{p} = (a, b, c, d, M_{s,\max})$ is not diagonal. Now \mathbf{p} is calculated as follows:

$$\mathbf{p} = \mathbf{Cz} + \mathbf{m} \quad (15)$$

where \mathbf{m} is the vector of the mean values of the parameters, \mathbf{C} is a unique lower triangular matrix such that $\mathbf{V} = \mathbf{C} \times \mathbf{C}^T$ and \mathbf{z} is our standard Gaussian random vector. Matrix \mathbf{C} is computed by recursive formulae (the ‘square root’ method). The Gaussian random deviates were produced using the polar Box–Muller transform as described by Marsaglia (1972). The average values of the standard errors in a and b and their covariance, as estimated from the application of equation (13) to the data (to be presented later), were 0.17, 0.03, and -0.005 , respectively, for the three zones in central Greece. A value of 0.35 was assigned to the standard error in $M_{s,\max}$. As the slope of equation (4) was held fixed when it was applied to the data, the total rms error, equal to 0.26, was assigned to the standard error, σ_d , in d . The standard error, σ_c , in c was taken equal to half the value of the last important digit, that is, 0.05. The covariance, σ_{cd} , of c and d was calculated as

$$\sigma_{cd} = r_{cd} \times \sigma_a \times \sigma_b,$$

where $r_{cd}(= -0.95)$ is the correlation coefficient of c and d which was approximated by the corresponding value of the least-squares solution.

Equation (15) was repeatedly applied in order to find new values of a , b , c , d and $M_{s,\max}$ which were used in order to estimate new values of \dot{M}_0 . Further analysis showed that the logarithm of \dot{M}_0 approximately follows a Gaussian distribution, with mean value being the one calculated by equation (15) and average standard deviation equal to 0.52 which corresponds to an error factor of 3.3 in \dot{M}_0 .

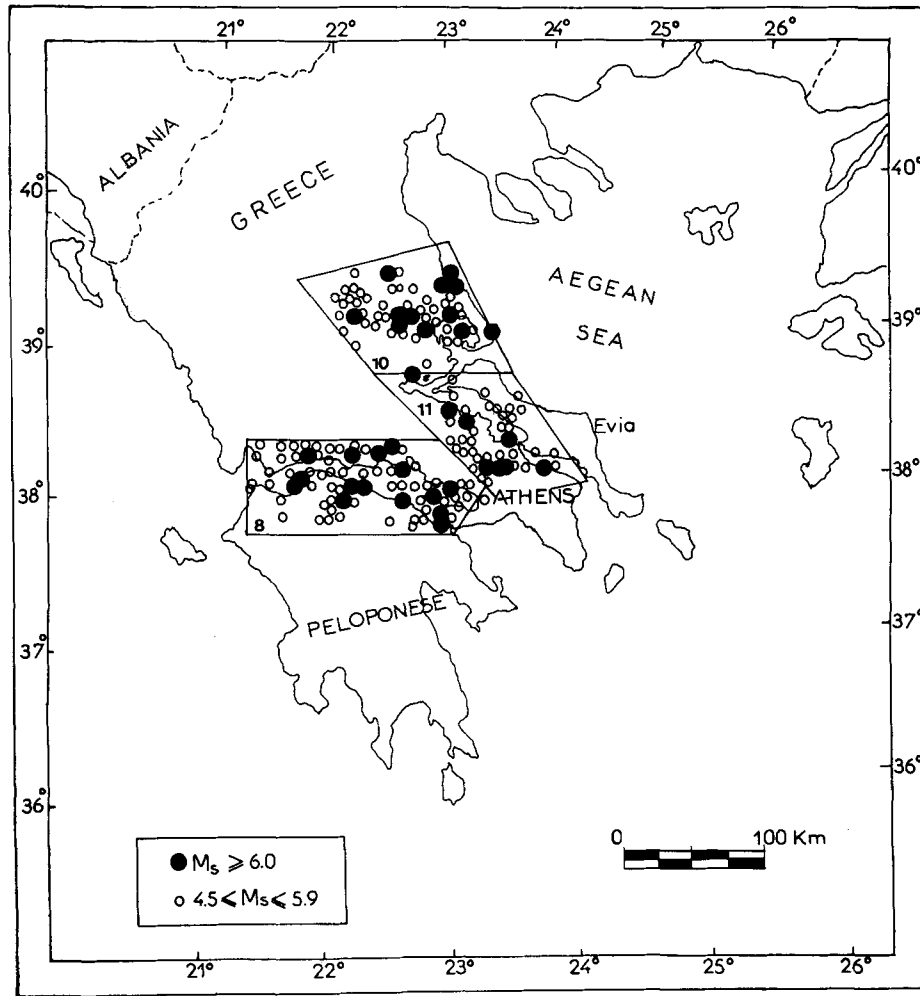


Figure 1. The area of central Greece studied, the seismic zones and the seismicity (complete data).

3.2 Errors in \bar{F}

From equations (3), (4) and (6) we conclude that errors in \bar{F} are due to errors in c , d and in the M_s , ϕ , δ and λ of each earthquake. However, using these equations, it is easy to show that:

$$\frac{\partial \bar{F}}{\partial d} = \ln 10 \frac{\sum_{n=1}^N M_0^n (F^n - \bar{F})}{\bar{F} \sum_{k=1}^N M_0^k} = 0, \quad (16)$$

and

$$\frac{\partial \bar{F}}{\partial c} = \ln 10 \frac{\sum_{n=1}^N M_0^n (F^n - \bar{F}) M_s^n}{\bar{F} \sum_{k=1}^N M_0^k} \approx 0, \quad (17)$$

if the magnitudes, M_s^n , of the focal mechanisms are of the same order. We can therefore consider errors introduced only by M_s^n and focal mechanism parameters. Since the errors in M_s^n , ϕ , δ and λ can be considered to be uncorrelated (diagonal \mathbf{V} matrix), we introduce Gaussian deviation in each of these parameters. The standard error in M_s^n was taken equal to 0.25 and a value of 10° was assigned

to the standard error of ϕ , δ and λ . New values were found for the elements of \bar{F} and analysis showed that they approximately followed a Gaussian distribution. These results (to be presented later) showed that errors in \bar{F} have very little influence on \dot{M} when compared to those introduced by \dot{M}_0 , that is, the error in the magnitude of the strain and velocity rates is determined by the error factor in \dot{M}_0 . The influence of \bar{F} is observed only in the direction of the eigenvalues of velocity and strain rate tensor (to be presented later) where errors in \dot{M}_0 have no effect.

4 RATES OF DEFORMATION IN CENTRAL GREECE

4.1 The seismic zones

The area of Greece has been separated into 26 seismic zones of shallow earthquakes on the basis of a large number of criteria (Papazachos 1990). The area of central Greece, which is studied here, represents the zones with numbers 8, 10 and 11, and covers the area of Patraikos–Corinthiakos Gulfs (zone 8), the area of Thessalia (zone 10), and the area of Atalanti–Evia and the surroundings (zone 11). Fig. 1 shows the area studied and the complete data for each zone. Information on the surface wave magnitudes and on the

Table 1. Information on the parameters used in the calculations: zone limits, time, t , since when each data sample is complete and corresponding minimum magnitude, M_{\min} , azimuth, ξ , of the maximum axis of the zone, maximum magnitude, $M_{s,\max}$, horizontal dimensions, l_1 , l_2 (in km) of the zone, parameters, a and b of the Gutenberg–Richter relation and moment rate, \dot{M}_0 (in 10^{25} dyn cm yr $^{-1}$).

Zone	t	M_{\min}	ξ	$M_{s,\max}$	l_1	l_2	a	b	\dot{M}_0
8									
37.90,21.30	1748	6.6	101	7.0	163	57	5.18	1.05	0.48
37.90,23.00	1858	6.0							
38.20,23.30	1901	5.5							
38.50,22.90	1911	5.0							
38.50,21.30	1965	4.5							
10									
38.95,22.35	1901	5.5	98	7.0	119	55	3.96	0.82	0.85
38.95,23.50	1911	5.0							
39.80,23.00	1965	4.5							
39.55,21.70									
11									
38.10,23.30	1758	6.8	108	7.0	117	77	4.18	0.92	0.31
38.20,24.10	1874	6.0							
38.95,23.50	1901	5.5							
38.95,22.35	1965	4.5							

epicentres of the earthquakes plotted in Fig. 1 were taken from the catalogue of Comninakis & Papazachos (1986) for the period 1901–85 and from the monthly bulletins of the National Observatory of Athens and of the Geophysical Laboratory of the University of Thessaloniki for the period 1986–90. For the historical earthquakes (before the present century) such information was taken from the book of Papazachos & Papazachou (1989).

Table 1 gives information on the parameters used for each seismic zone. The geographic coordinates of the points which define each zone are given on the first column. The second and third column show the time (year) since when the data are complete for each magnitude range, and the minimum magnitude of this range, respectively. For the first zone (8), for example, the complete data sets are all earthquakes with $M_s \geq 6.6$, 6.0, 5.5, 5.0 and 4.5 for the periods 1748–1990, 1858–1990, 1901–90, 1911–90 and 1965–90, respectively. This completeness has been determined for each zone on the basis of information given in the catalogues, which have been used as data sources and of plots of the frequency–magnitude relation for each magnitude range. The fourth column of Table 1 shows the angle, ξ , of the longest direction of the zone with North. The magnitude, $M_{s,\max}$, i.e. the maximum magnitude ever observed in each zone, is given in the fifth column. The length, l_1 , and the width, l_2 , for each zone are listed in the sixth and seventh column of this table. The parameters a and b of the Gutenberg–Richter relation are shown in the eighth and ninth column, respectively. Finally, the last column of Table 1 lists the seismic moment rate calculated in a way previously discussed.

As it is seen in Fig. 1, in some cases the area covered by epicentres does not necessarily cover the whole seismic zone. Since we are interested in the active part of each zone, and because for the purpose of the present paper we need to have zones of rectangular shape, we assumed that the epicentral area of each zone has such shape. Thus, the length, the width and the azimuth of the zones were

calculated as follows. Using the complete data set we calculated the coordinates of the centre of the zone which we choose as the centre of a coordinate system with x and y axes parallel to NS and EW direction, respectively. Assuming that the earthquakes in each zone generally follow a linear pattern, we calculated a least-squares best-fit line for each zone. The projections of the most distant epicentres, from the centre of the zone, onto this line define the length, l_1 , of the zone. The width, l_2 , of the zone is taken to be 4σ , where σ is the standard deviation of the earthquake epicentres from the line and, finally, the azimuth, ξ , is taken to be the azimuth of the line with North. The value of l_3 (depth extent of the seismogenic layer) was taken to be 15 km for all zones. This value was chosen based on the results of previous work (Taymaz *et al.* 1991; Karacostas & Papazachos 1991; Kiratzi, Wagner & Langston 1991).

4.2 The moment–magnitude relation

The values $c = 1.5$ and $d = 15.89$ for the constants of equation (4) have been used in the relations (12). These values have been determined using data on seismic moments determined by the inversion of body waves and on surface wave magnitudes for earthquakes of the Aegean and its surroundings. These data are listed in Kiratzi, Papadimitriou & Papazachos (1991). Some of the data were excluded, that is, those with depth ≥ 50 km, magnitude ≤ 5.5 , as well as seismic moments determined by the inversion of surface waves. Fig. 2 is a plot of the logarithm of the seismic moment versus the surface wave magnitude. Instead of performing a least-squares fit to the data, we preferred to keep the slope of the line equal to 1.5, which was previously suggested (Hanks & Kanamori 1979), and calculate the intersection of the line with the y -axis (value of $d = 15.89$). This is not a crude assumption, since this value of the slope was determined, independently, for the same area

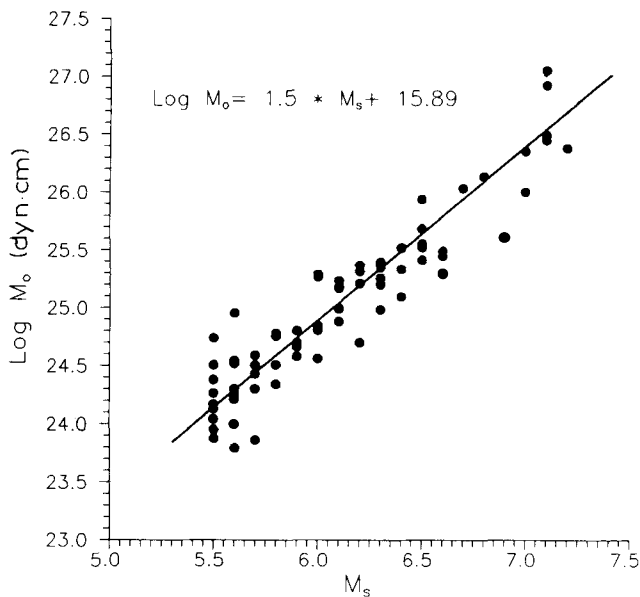


Figure 2. Plot of the logarithm of seismic moment (determined by the inversion of body waves) versus surface wave magnitude for earthquakes in the Aegean area (data from Kiratzi, Papadimitriou & Papazachos 1991).

(Papazachos & Papazachou 1989). The proposed relation

$$\log M_0 = 1.5M_s + 15.89 \quad (18)$$

fits the data for the Aegean area satisfactorily and we prefer to use this relation to any other global one.

4.3 Fault-plane solutions

Table 2 lists the most reliable fault-plane solutions for the area of central Greece studied here. Various sources have been used and are accordingly referenced. In this table for each event are given: a code number, the date and time of occurrence, the epicentral coordinates, the depth and the scalar seismic moment if determined by waveform modelling, and finally the strike, dip and rake of the corresponding fault plane.

Table 2. Fault-plane solutions of the earthquakes used in the analysis.

No	Date	Time h:m:s	Epicentral coordinates $\phi^{\circ}\text{N}$ $\lambda^{\circ}\text{E}$		D (Km)	M_0 $\times 10^{24}$ dyncm	Ms	Str	dip	rake	Ref
1	Jul 6, 1965	03:18:42	38.4	22.4			6.3	90	74	-115	1
2	Feb 5, 1966	02:01:45	39.1	21.7	5	5.0	6.2	103	23	-75	2
3	Apr 8, 1970	13:50:28	38.3	22.6	9	9.1	6.2	75	67	-94	3
4	Jul 9, 1980	02:10:20	39.3	22.9			5.6	82	42	-79	4
5	Jul 9, 1980	02:11:57	39.3	22.9			6.5	81	40	-90	4
6	Jul 9, 1980	02:35:52	39.2	22.6			6.1	81	40	-90	4
7	Feb 24, 1981	20:53:37	38.2	23.0	12	87.5	6.7	264	42	-80	5
8	Feb 25, 1981	02:35:54	38.2	23.1	8	39.7	6.4	241	44	-85	5
9	Mar 4, 1981	21:58:07	38.2	23.3	7	27.0	6.3	230	45	-105	5
10	Apr 30, 1985	18:14:13	39.3	22.8	11	3.0	5.8	77	50	-105	5

1 McKenzie (1972),

2 Anderson & Jackson (1987),

3 Liotier (1989),

4 Papazachos *et al.* (1983),

5 Taymaz *et al.* (1991).

Fig. 3 shows the focal mechanisms of the earthquakes listed in Table 2. It is seen, that all these events are caused by normal faulting, showing extension in an about NNW-SSE direction. It is obvious that these events can be regarded as belonging to the same seismotectonic unit, or, as previously stated, to the same seismic belt.

4.4 Rates of deformation

Following the formulation developed earlier in this paper, the moment rate tensor, the strain rate tensor as well as the corresponding velocity tensor were calculated for each zone separately as these are shown in Fig. 1.

The components of the tensor F_{ij} for the whole seismic belt are:

$$\begin{array}{ccc} 0.83 \pm 0.07 & -0.18 \pm 0.08 & -0.07 \pm 0.13 \\ -0.18 \pm 0.08 & 0.08 \pm 0.05 & 0.05 \pm 0.07 \\ -0.07 \pm 0.13 & 0.05 \pm 0.07 & -0.91 \pm 0.05. \end{array}$$

The uncertainties shown in this tensor are calculated in the way described previously.

In the following, the deformation rates are given for each zone.

4.4.1 Zone 8 (Corinthiakos-Patraikos Gulfs)

This zone covers the area of the Corinthiakos-Patraikos Gulfs. The most recent earthquakes which occurred in the area are the 1981 series of events, which produced major faulting in the field. A total of 148 earthquakes with well established parameters were used in this zone. The moment rate release, as calculated by equation (14), is equal to 4.8×10^{24} dyn cm yr⁻¹.

The elements of the strain rate tensor in the coordinate system of the zone (azimuth 101°) are as follows:

$$\begin{array}{ccc} 1.17 & 2.08 & 0.43 \\ 2.08 & 4.87 & 0.39 \\ 0.43 & 0.39 & -6.04 \end{array} \times 10^{-8} \text{ yr}^{-1}.$$

The components of the velocity tensor in the coordinate

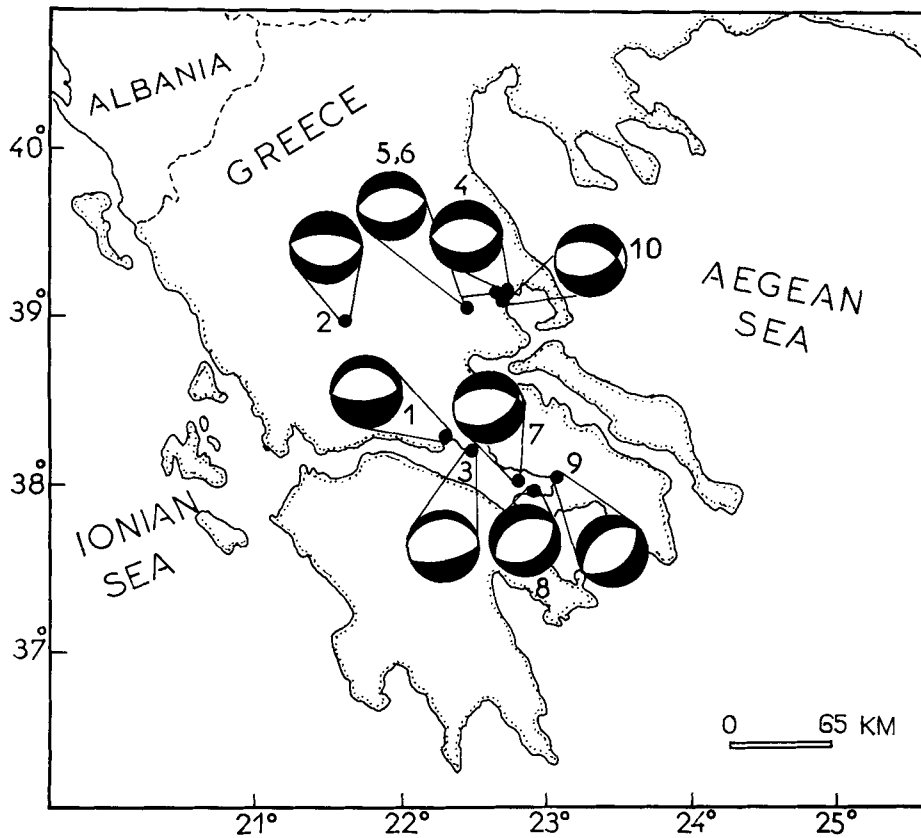


Figure 3. The fault-plane solutions of the earthquakes used in the analysis.

system of the zone are:

1.91	2.36	0.13	
2.36	2.75	0.12	mm yr ⁻¹ .
0.13	0.12	-0.91	

The corresponding components of the velocity tensor in the coordinate system used (1: North, 2: East, 3: Down) are:

3.63	-2.01	-0.14	
-2.01	1.03	0.10	mm yr ⁻¹ ,
-0.14	0.10	-0.91	

and its eigenvalues and associated eigenvectors are:

<i>v</i> (mm yr ⁻¹)	4.73	-0.06	-0.91
Plunge°	1.8 ± 3.0	1.6 ± 9.6	-87.6 ± 5.2
Azimuth°	151.5 ± 7.6	61.4 ± 10.7	109.3

It is observed that the dominant mode of deformation in this zone is expressed as extension in the NNW-SSE direction at a rate of 4.7 mm yr⁻¹. It is also interesting to note the existence of a considerable vertical motion, at a rate of about 1 mm yr⁻¹, expressed as crustal thinning previously observed by Jackson, King & Vita-Finzi (1982).

4.4.2 Zone 10 (Thessalia)

This zone covers the area of Thessalia which has been the site of intense seismic activity during the present century (1954, 1955, 1957, 1980). A total of 73 earthquakes with

well-established parameters were used. The moment rate release is equal to 8.5×10^{24} dyn cm yr⁻¹. The elements of the strain rate in the coordinate system of the zone are:

2.12	4.22	0.94	
4.22	11.78	0.97	$\times 10^{-8}$ yr ⁻¹ .
0.94	0.97	-13.91	

The components of the velocity tensor in the same system are:

2.52	4.63	0.28	
4.63	6.46	0.29	mm yr ⁻¹ .
0.28	0.29	-2.09	

The corresponding components of the velocity tensor in the coordinate system 1: North, 2: East, 3: Down are:

7.63	-3.94	-0.33	
-3.94	1.35	0.24	mm yr ⁻¹ ,
-0.33	0.24	-2.09	

and its eigenvalues and associated eigenvectors are:

<i>v</i> (mm yr ⁻¹)	9.54	-0.54	-2.10
Plunge°	2.0 ± 3.3	2.7 ± 11.8	-86.6 ± 6.5
Azimuth°	154.3 ± 7.7	64.2 ± 7.8	100.0

It is observed that the deformation of this zone is taken up by extension in a NNW-SSE direction at a rate of 9.5 mm yr⁻¹. A considerable vertical motion of 2 mm yr⁻¹ is also observed.

4.4.3 Zone 11 (Atalanti–western Evia)

In this area, the most important feature is the Atalanti fault. This a major normal fault which has ruptured in the past (1894 $M_s = 7.0$). Its proximity to the city of Athens makes this fault very important in terms of seismic hazard. A total of 37 earthquakes were used in the analysis. The moment rate release is 3.1×10^{24} dyn cm yr⁻¹.

The elements of the strain rate tensor in the coordinate system of the zone (azimuth 108°) are:

$$\begin{array}{ccc} 1.08 & 1.57 & 0.31 \\ 1.57 & 2.83 & 0.22 \\ 0.31 & 0.22 & -3.90 \end{array} \times 10^{-8} \text{ yr}^{-1}.$$

The components of the velocity tensor in the same system are:

$$\begin{array}{ccc} 1.25 & 2.43 & 0.09 \\ 2.43 & 2.18 & 0.07 \\ 0.09 & 0.07 & -0.59 \end{array} \text{ mm yr}^{-1}.$$

The corresponding components of the velocity tensor in the coordinate system used (1:North, 2:East, 3:Down) are:

$$\begin{array}{ccc} 3.50 & -1.72 & -0.09 \\ -1.72 & -0.06 & 0.07 \\ -0.92 & 0.07 & -0.59 \end{array} \text{ mm yr}^{-1},$$

and its eigenvalues and associated eigenvectors are:

v (mm yr ⁻¹)	4.19	-0.76	-0.58
Plunge°	1.3 ± 2.3	-9.4 ± 12.0	80.5 ± 7.0
Azimuth°	158.0 ± 5.0	68.2 ± 21.0	60.0

It is seen that the dominant mode of deformation in the zone, is extension at an azimuth N22°W and at a rate of 4.2 mm yr⁻¹. A vertical contraction around 0.6 mm yr⁻¹ also occurs.

5 CONCLUSIONS AND DISCUSSION

Improving the determination of the moment rate tensor, \dot{M} , is important for a reliable estimation of active deformation. Here, we suggest an independent determination of the scalar moment rate, \dot{M}_0 , on which the 'size' of the deformation depends, and of the representative focal mechanism tensor, \bar{F} , on which the 'shape' of the deformation depends. This exploits the fact that: (a) independent determination of \dot{M}_0 can be based on more data, which include present century instrumental information on large and small earthquakes and historical information on large earthquakes; (b) independent determination of \bar{F} can be based on a larger number of reliable fault-plane solutions of a broader seismic region where faulting (strike, dip, rake) does not vary considerably.

A detailed error analysis, based on a Monte Carlo numerical method, shows that errors in \bar{F} have little influence in the uncertainty of the magnitude of the deformation when compared to those introduced by \dot{M}_0 which are of a factor of 3. Errors in \bar{F} , however, influence the direction of deformation where errors in \dot{M}_0 have no effect.

Since the main source of errors in the magnitude of the deformation comes from errors in \dot{M}_0 and the calculation of this quantity in the present paper is based on relation (14), it is of interest to compare the results of this calculation with results based on the calculation of \dot{M}_0 by the use of data of only strong earthquakes ($M_s \geq 6.0$) and direct application of relation (18). In the three zones 8, 10 and 11 the data for $M_s \geq 6.0$ are complete since 1858, 1901 and 1874 (see Table 1), respectively, and the corresponding number of such strong shocks which occurred since these years are 10, 11 and 6, respectively. This calculation results in the values of 3.0 (in units of 10^{24} dyn cm yr⁻¹), 6.7 and 2.7 for the corresponding moment rates for the three seismic zones, while application of relation (14) gave 4.8, 8.5 and 3.1, respectively, that is, higher values. This is a plausible result because relation (14) gives the moment release by 'all' earthquakes. It also indicates that almost 75 per cent of the total moment is released by large ($M_s \geq 6.0$) earthquakes.

The maximum velocity rates in all three zones (8, 10 and 11) have a NNW–SSE trend, are extensional, and their values are 4.7, 9.5 and 4.2 mm yr⁻¹, respectively. Taking into consideration the uncertainties involved, their average value, 6 mm yr⁻¹, can be considered as a representative value for central Greece. This is in good agreement with the results of Ambraseys & Jackson (1990) who estimated that earthquakes with $M_s \geq 5.8$ which occurred in central Greece between 1890 and 1988 can account for about 450–700 mm of north–south extension. Our extensional velocity rate, due to seismic energy release, is about half the total velocity rate calculated by Billiris *et al.* (1991) on the basis of geodetic observations in a part of central Greece. These observations come from a triangulation network, that was in operation for the period 1900–88 and indicates 1 m of north–south extension during this period. It seems, that at least for this area, about 50 per cent of the accumulation of strain is released seismically.

The vertical velocity rates indicate contraction for all three zones and their values are 0.9, 2.0 and 0.6 mm yr⁻¹, respectively. Taking into consideration the uncertainties involved, their average, 1 mm yr⁻¹, can be considered as the representative value of the vertical seismic deformation for central Greece.

A computer program which makes all calculations concerning the present study has been prepared and can be obtained upon request.

ACKNOWLEDGMENTS

The authors would like to express their sincere gratitude to Professor B. Papazachos of the Geophysical Laboratory of the University of Thessaloniki, for his guidance throughout this work. Drs E. Papadimitriou and G. Karakaisis are thanked for their careful reading of the original manuscript. Finally, we would like to thank the two anonymous reviewers for their constructive criticism.

REFERENCES

- Aki, K. & Richards, P., 1980. *Quantitative Seismology: Theory and Methods*, Freeman, San Francisco, California, 557 pp.
 Ambraseys, N. N. & Jackson, J. A., 1990. Seismicity and associated

- strain of central Greece between 1890 and 1988, *Geophys. J. Int.*, **101**, 663–709.
- Anderson, H. & Jackson, J., 1987. Active tectonics of the Adriatic Region, *Geophys. J. R. astr. Soc.*, **91**, 937–983.
- Billiris, H., Paradisis, D., Veis, G., England, P., Featherstone, W., Parsons, B., Cross, P., Rands, P., Rayson, M., Sellers, P., Ashkenazi, V., Davison, M., Jackson, J. & Ambraseys, N., 1991. Geodetic determination of tectonic deformation in central Greece from 1900 to 1988, *Nature*, **305**, 124–129.
- Comninakis, P. & Papazachos, B., 1986. A catalogue of earthquakes in the Aegean and surrounding area for the period 1901–1985, *Publ. Geophys. Lab. Univ. of Thessaloniki*, **1**, 167 pp.
- Ekstrom, G. & England, P., 1989. Seismic strain rates in regions of distributed continental deformation, *J. geophys. Res.*, **94**, 10 231–10 257.
- Hanks, T. & Kanamori, H., 1979. A new moment-magnitude scale, *J. geophys. Res.*, **84**, 2348–2350.
- Jackson, J. & McKenzie, D., 1988a. The relationship between plate motions and seismic moment tensors, and the rates of active deformation in the Mediterranean and Middle East, *Geophys. J.*, **93**, 45–73.
- Jackson, J. & McKenzie, D., 1988b. Rates of active deformation in the Aegean Sea and surrounding regions, *Basin Res.*, **1**, 121–128.
- Jackson, J., King, G. & Vita-Finzi, C., 1982. The neotectonics of the Aegean: an alternative view, *Earth planet. Sci. Lett.*, **61**, 303–318.
- Karacostas, B. & Papazachos, B., 1991. A catalogue of earthquakes in Greece and the surrounding area for the time period 1970–1987, *Publ. Geophys. Lab. Univ. of Thessaloniki*, **6**, 1–49.
- Kiratzi, A., 1991. Rates of crustal deformation in the north Aegean trough–north Anatolian fault deduced from seismicity, *Pageoph*, **136**, 421–432.
- Kiratzi, A., Papadimitriou, E. & Papazachos, B., 1991. Seismic moments and focal depths of the earthquakes of the Aegean area determined by waveform modeling, *Publ. Geophys. Lab. Univ. of Thessaloniki*, **10**, 1–14.
- Kiratzi, A., Wagner, G. & Langston, C., 1991. Source parameters of some large earthquakes in northern Aegean determined by body waveform inversion, *Pageoph*, **135**, 515–527.
- Kostrov, V., 1974. Seismic moment and energy of earthquakes, and seismic flow of rock, *Izv. Acad. Sci. USSR Phys. Solid Earth*, **1**, 23–44.
- Liotier, Y., 1989. Modelisation des ondes de volume ses seismes de l'arc Egeen, *Formation de 3^e Cycle*, UFR de Mechanique, Universite Joseph Fourier de Grenoble 1.
- Marsaglia, G., 1972. *Applications of Number Theory to Numerical Analysis*, Academic Press, New York.
- McKenzie, D., 1972. Active tectonics of the Mediterranean region, *Geophys. J. R. astr. Soc.*, **30**, 109–185.
- Milne, W. G. & Davenport, A. G. 1969. Determination of earthquake risk in Canada, *Bull. seism. Soc. Am.*, **59**, 729–754.
- Molnar, P., 1979. Earthquake recurrence intervals and plate tectonics, *Bull. seism. Soc. Am.*, **69**, 115–133.
- Papazachos, B. C., 1990. Seismicity of the Aegean and surrounding area, *Tectonophysics*, **178**, 287–308.
- Papazachos, B. & Papazachou, C., 1989. *The Earthquakes of Greece*, Ziti Publications, Thessaloniki, 356 pp.
- Papazachos, B. C., Kiratzi, A. A., Papaioannou, Ch. A. & Panagiotopoulos, D. G., 1990. Average regional seismic strain release rates in the Patraikos–Saronikos Gulfs (central Greece) based on historical and instrumental data, *Conference of the Geological Society of Greece Thessaloniki 1990*, 1–15.
- Papazachos, B. C., Panagiotopoulos, D. G., Tsapanos, T. M., Mountrakis, D. M. & Dimopoulos, G. Ch., 1983. A study of the 1980 summer sequence in the Magnesia region of Central Greece, *Geophys. J. R. astr. Soc.*, **75**, 155–168.
- Scholz, C. H., 1986. The frequency–magnitude relation of microfracturing in rock and its relation to earthquakes, *Bull. seism. Soc. Am.*, **58**, 399–415.
- Taymaz, T., Jackson, J. & McKenzie, D., 1991. Active tectonics of the north and central Aegean Sea, *Geophys. J. Int.*, **106**, 433–490.
- Tselentis, G. & Makropoulos, C., 1986. Rates of crustal deformation in the gulf of Corinth (central Greece) as determined from seismicity, *Tectonophysics*, **124**, 55–66.